

Influence of Host Lattice Cations on the Charge Transfer Band (CTB) of Scheelite Host Lattices

J. Mastan^a, G. R. Patta^a, U.V. Varadaraju^b and S. Asiri Naidu^{a*}

^aDepartment of Chemistry, Rajiv Gandhi University of Knowledge Technologies-IIIT Nuzvid, Andhra Pradesh, India

^bDepartment of Chemistry, Indian Institute of Technology Madras, Chennai, India

Abstract

The $\text{Na}_5\text{Y}_{0.95}\text{Eu}_{0.05}(\text{WO}_4)_{4-x}(\text{MoO}_4)_x$ [$x = 0-4$], $\text{Na}_5\text{Y}_{1-x}\text{Eu}_x(\text{MO}_4)_4$ [$M = \text{W}, \text{Mo}$], $\text{Na}_5\text{La}_{1-x}\text{Eu}_x(\text{MO}_4)_4$ [$M = \text{W}, \text{Mo}$] and $\text{Na}_5\text{Gd}_{1-x}\text{Eu}_x(\text{MO}_4)_4$ [$M = \text{W}, \text{Mo}$] compositions have been synthesized by solid-state reaction method. In case of molybdate host lattices the wavelength maximum (λ_{max}) of charge transfer band shifts towards shorter wavelength, where as in tungstate host lattices the wavelength maximum (λ_{max}) of charge transfer band shifts towards longer wavelength with increasing Eu^{3+} concentration.

1. Introduction

In double molybdates with scheelite related structure, the alkali ions and rare earth ions are randomly distributed over the available cation sites, the different cations with different radii in the scheelite host lattice would induce some change in the sub-lattice structure around the activator ions, even change the host lattice structure and hence results in different photoluminescent properties [1, 2]. In particular, the scheelite type rare earth sodium double molybdates $\text{Na}_5\text{RE}(\text{MoO}_4)_4$ or tungstates $\text{Na}_5\text{RE}(\text{WO}_4)_4$, are considered to be efficient luminescent host lattices [3, 4]. It has been reported recently, a near-UV (393 nm) convertible red phosphor of formula $\text{NaY}_{0.95}\text{Eu}_{0.05}(\text{WO}_4)_{2-x}(\text{MoO}_4)_x$ ($x = 0-2$) and the phosphor $\text{AgGd}_{0.95}\text{Eu}_{0.05}(\text{WO}_4)_{2-x}(\text{MoO}_4)_x$ ($x = 0-2$) under 465 nm (blue spectral region) excitation wavelength for white light emitting diodes. And also it was observed that the absorption edge of the O-W/Mo charge transfer band (CTB) shifted to longer wavelength by mixing the anionic part in that host lattices [5, 6]. A similar phenomenon is observed in $\text{Ba}_2\text{Ca}_{0.8}\text{Li}_{0.1}\text{Eu}_{0.1}\text{Mo}_{1-x}\text{W}_x\text{O}_6$ double perovskites [7]. $\text{Eu}^{3+}-\text{O}^{2-}$ CTB is strongly related to the covalency between O^{2-} and Eu^{3+} ions reported in the literature [8-10]. It has been reported in the literature that the wavelength maximum of O-Mo CTB exhibits a blue shift with the increasing of Eu^{3+} concentration [11]. None of the literature reports dealt with the relative comparison of CTB shifts in both the tungstate and molybdate scheelites and other host lattices with the increase of Eu^{3+} concentration.

With this view, in the present study, we have synthesized $\text{Na}_5\text{Y}_{1-x}\text{Eu}_x(\text{MO}_4)_4$ ($M = \text{W}, \text{Mo}$), $\text{Na}_5\text{La}_{1-x}\text{Eu}_x(\text{MO}_4)_4$ ($M = \text{W}, \text{Mo}$) and $\text{Na}_5\text{Gd}_{1-x}\text{Eu}_x(\text{MO}_4)_4$ ($M = \text{W}, \text{Mo}$) phases and studied their excitation spectra. The influence of constituent cations on the λ_{max} of CTB is established.

2. Experimental

$\text{Na}_5\text{Y}_{1-x}\text{Eu}_x(\text{MO}_4)_4$ ($x = 0.05, 0.1, 0.3, 0.5, 0.7$ and 1.0 , $M = \text{W}, \text{Mo}$) [12], $\text{Na}_5\text{La}_{1-x}\text{Eu}_x(\text{MO}_4)_4$ ($x = 0.05, 0.1, 0.5, 1.0$; $M = \text{W}, \text{Mo}$) [13], $\text{Na}_5\text{Gd}_{1-x}\text{Eu}_x(\text{MO}_4)_4$ ($x = 0.05, 0.1, 0.5, 1.0$; $M = \text{W}, \text{Mo}$) [14, 15] phases are prepared by solid state reaction as reported in the literature. The starting materials used for Y and Gd-phases are, Na_2CO_3 , Ln_2O_3 ($\text{Ln} = \text{Y}, \text{La}, \text{Eu}$, 99.99%, Indian Rare Earths), WO_3 (99.5%, Aldrich), MoO_3 . For La-phases $(\text{NH}_4)_6\text{Mo}_7\text{O}_{24} \cdot 4\text{H}_2\text{O}$ (AR grade, CDH), $(\text{NH}_4)_{10}\text{H}_2\text{W}_{12}\text{O}_{42} \cdot x\text{H}_2\text{O}$ (AR grade, CDH), NaHCO_3 (AR grade, SRL), Ln_2O_3 ($\text{Ln} = \text{La}, \text{Eu}$, 99.99%, Indian Rare Earths) are used. Y_2O_3 , Gd_2O_3 and La_2O_3 , were preheated at 900 °C overnight. The stoichiometric precursors were weighed accurately and were mixed together using an agate mortar and pestle. During grinding, a small amount of ethanol was added in order to mix the precursors homogeneously subjected to the following heat treatment protocol: 600 °C for 8h with one

intermediate grinding for La series of compounds; 2 days for 500 °C and 5 days for 800 °C with several intermediate grindings for the Y and Na₅Gd_{1-x}Eu_x(MoO₄)₄ series of compounds; 600 °C for 5h for Na₅Gd_{1-x}Eu_x(WO₄)₄ series of compounds.

Powder X-ray diffraction data were recorded for all the above samples, using a Panalytical X'pertPro X-ray diffractometer with a CuK α source ($\lambda = 1.5418 \text{ \AA}$). No impurity phases were detected. The crystallographic data of NaGd(WO₄)₄ is not reported in the literature. Crystal structure of the parent NaGd(WO₄)₄ phase was refinement by the Rietveld method using the Fullprof program [16].

Excitation spectra were measured by using JASCO-3600 spectrophotometer. An R-60 glass filter was used while recording the excitation spectra to remove the lower order reflections of the emission wavelength. All measurements have been carried out at room temperature.

3. Results and discussion

It has been reported that the parent molybdate and tungstate compounds are isostructural and belongs to the tetragonal space group I4_{1/a} (Z = 4) with scheelite structure. In these structures two different sodium sites exist; (Na(2) with irregular six coordination and Na(1) with tetrahedral coordination) with respect to oxygen. Ln³⁺ ions occupy eight coordinated site (square prismatic) and Mo⁶⁺/W⁶⁺ occupy tetrahedral sites. The local site symmetry of Y³⁺ in these structures is S₄ (approximate D_{2d} symmetry). No impurity phases were detected in parent as well as in the Eu³⁺ contain phases establishing that the solid solutions are pure in nature (Figures not shown). The XRD patterns of the NaLn(MO₄)₄ (Ln = Y, Gd, La; M = W, Mo) phases show that all the compositions crystallize in the tetragonal structure with good crystallinity. The refined lattice parameters and the agreement factors are given in Table 1. The atomic parameters and distances of NaGd(WO₄)₄ are given in Tables 2 and 3, respectively. The observed, calculated and difference diffractograms of NaGd(WO₄)₄ are shown in Fig. 1.

Photoluminescence properties:

Figure. 2 shows Eu³⁺ excitation spectra of all Na₅Y_{1-x}Eu_x(MoO₄)₄ (x = 0.05, 0.1, 0.3, 0.5, 0.7, 1.0) phases recorded under 619 nm emission wavelength. The broad band in the region of 220 and 350 nm is attributed to the O Mo(Eu)/W(Eu) CTB (ligand to metal). However, O²⁻-Eu³⁺ charge transfer band is conspicuous in the excitation spectra, which may be due to overlap of charge transfer band with that of tungstate or molybdate moieties. The sharp lines in the range from 350-550 nm are intra-4f transitions of Eu³⁺. The intensity of O Mo(Eu)/W(Eu) CTB in the region of 220 and 350 nm increases with Eu³⁺ concentration. A clear observation from the excitation spectra is that the absorption maximums of CTB shifts towards lower wavelength side (blue shift) with increasing Eu³⁺ concentration. The trend of shifting λ_{max} of CTB with Eu³⁺ concentration is reported in Na₅La_{1-x}Eu_x(MO₄)₄ host lattice by Wang *et al.* [10]. Figure. 3 shows Eu³⁺ excitation spectra of all Na₅Y_{1-x}Eu_x(WO₄)₄ (x = 0.05, 0.1, 0.3, 0.5, 0.7, 1.0) phases recorded under 619 nm emission wavelength. The intensity of O W(Eu)/W(Eu) CTB in the region of 220 and 350 nm increases with Eu³⁺ concentration. A clear observation from the excitation spectra is that the absorption maxima of CTB shift towards higher wavelength side (red shift) with increasing Eu³⁺ concentration. A similar trend i.e., change in λ_{max} of CTB with Eu³⁺ concentration is observed in Na₅La_{1-x}Eu_x(MO₄)₄ (M = W, Mo) and Na₅Gd_{1-x}Eu_x(MO₄)₄ (M = W, Mo) host lattices (Figs. 4, 5, 6 & 7). From the above results it is clear that in all the presently studied molybdate host lattices the λ_{max} of CTB shifts towards shorter wavelength side, where as in case of all the tungstate host lattices the λ_{max} of CTB shifts towards longer wavelength side with increasing Eu³⁺ concentration.

It has been reported in the literature that the wavelength maximum of O Mo CTB exhibits a blue shift with the increasing of Eu³⁺ concentration [17]. The profound reason for this observation has not been discussed in that reported work. Guo *et al.* have been reported that the Eu³⁺ doped NaLn(MoO₄)₄ (Ln = Y, Gd, La) red phosphors are promising candidates for white light emitting diodes [18]. However, the authors have not revealed any observation regarding shifts of CTB in these host lattices. The O Eu³⁺ charge transfer excitation involves the promotion of electrons from 2p valence orbital of oxygen to 4f levels of Eu³⁺, and the CTB peak position is depends on the energy difference between O 2p valence band and 4f levels of Eu³⁺. Lin

et al., reported that the peak position of CTB depends on the length of the Eu-O bond: the shorter the Eu-O bond, the larger the energy difference between the 4f and O 2p electrons, consequently the CTB observed at higher energy position [19]. The average Eu-O bond distance in valerite type $\text{LuBO}_3:\text{Eu}^{3+}$ is longer than that of the calcite type $\text{LuBO}_3:\text{Eu}^{3+}$, leading to the red shift of Eu-O CTB in valerite type $\text{LuBO}_3:\text{Eu}^{3+}$ [20]. It is obvious that the two different crystal structures with different space groups having different bond distances which results in the shifting of CTB. In the present work the entire studied host lattices are belongs to the same space group except a change in the constituent cations, which eventually influence the CTB shifts we expect. The bond distances of all the parent host lattices have been tabulated in the Table I. However, we tried correlating the observed discrepancy of the CTB shifts with the Ln-O bond distances, but the change of Ln-O bond distances is not uniform as shown in the table 1.

4. Conclusion

The dependence of Eu^{3+} excitation spectra in sodium lanthanum tungstate/molybdate solid solutions with scheelite related structure is studied. The CTB maximum in molybdates shifts towards shorter wavelength (blue shift), whereas in the case of tungstates CTB maximum shifts towards longer wavelength (red shift) with increase in Eu^{3+} concentration in all the sodium (yttrium, lanthanum, gadolinium) molybdate/tungstate host lattices. The WO_4^{2-} and MoO_4^{2-} moieties influence the λ_{max} of CTB in these scheelite host lattices.

References

1. Z. Wang, H. Liang, L. Zhou, H. Wu, M. Gong and Q. Su, *J. Alloys Compds.*, **432**, 308 (2007).
2. V. K. Trunov, T. A. Berezina, A. A. Evdokimov, V. K. Ishunin and V. G. Krongauz, *Russ. J. Inorg. Chem.*, **23**, 2645 (1978).
3. J. Huang, J. Loriers, P. Procher, G. Teste De Sagey, P. Caro and C. Lecy-Clememt, *J. Chem. Phys.*, **80**, 6204 (1984).
4. J. Pan, L. Yau, L. Chen, G. Zhao, G. Zhou and C. Guo, *J. Lumn.*, **40&41**, 856 (1988).
5. S. Neeraj, N. Kijima and A. K. Cheetham, *Chem. Phys. Lett.*, **387**, 2 (2004).
6. V. Sivakumar and U. V. Varadaraju, *J. Electrochem. Soc.*, **152**, H168-H171(2005).
7. S. Ye, C.-H. Wang, Z.-S. Liu, J. Lu, X.-P. Jing, *Appl. Phys. B*, **91**, 551–557 (2008).
8. T. Igarashi, M. Ihara, T. Kusunoki, K. Ohno, T. Isobe, M. Senna, *Appl. Phys. Lett.* **76**, 159-1551 (2000).
9. M. Jia, J. Zhang, S. Lu, J. Sun, Y. Luo, X. Ren, H. Song, X-j. Wang, *Chem. Phys. Lett.* **384**, 193–196 (2004).
10. Z. Lu, L. Chen, Y. Tang, Y. Li, *J. Alloys Compd.* **387**, L1-L4 (2005).
11. Z. Wang, H. Liang, J. Wang, M. Gong and Q. Su, *Appl. Phys. Lett.* **89**, 071921 (2006)
12. N.J. Stedman, A.K. Cheetham and P.D. Battle, *J. Mater. Chem.* **4**, 707-711 (1994).
13. Z. Wang, H. Liang, J. Wang, M. Gong and Q. Su, *Appl. Phys. Lett.* **89**, 071921 (2006).
14. J.P.M. Van Vliet and G. Blasse, *J. Solid State. Chem.* **85**, 56-64 (1990).
15. D. Zhao, W.-D. Cheng, H. Zhang, S.-P. Huang, M. Fang, W.-L. Zhang, S.-L. Yang, J. Mol. Struct. **919**, 178–184 (2009).
16. Fullprof Suite Program (1.00) – version February 2007, J. R. Carvajal (ILL, France), T. Roisnel (LCSIM, CNRS, France), J. G. Platas (ULL, Spain), L. C. Chapon (ISIS, RAL, UK).
17. Z. Wang, H. Liang, J. Wang, M. Gong and Q. Su, *Appl. Phys. Lett.* **89**, 071921 (2006).
18. C. Guo, F. Gao, Y. Xu, L. Liang, F. G. Shi and B. Yan, *J. Phys. D: Appl. Phys.* **42**, 095407 (2009).
19. Lin, J. H.; You, L. P.; Lu, G. X.; Yang, L. Q.; Su, M. Z. *J. Mater. Chem.* **8**, 1051 (1998).

20. Y. Li, J. Zhang, X. Zhang, Y. Luo, S. Lu, X. Ren, X. Wang, L. Sun and C. Yan, *Chem. Mater.* **21**, 468–475 (2009).

Figure captions

Figure 1. X-ray powder diffraction patterns of $\text{Na}_5\text{Gd}(\text{WO}_4)_4$ (observed, calculated and difference patterns are represented with dots, bold line and solid line, respectively; positions of Bragg reflections with vertical bars).

Figure 2. Excitation spectra of $\text{Na}_5\text{Y}_{1-x}\text{Eu}_x(\text{MoO}_4)_4$.

Figure 3. Excitation spectra of $\text{Na}_5\text{Y}_{1-x}\text{Eu}_x(\text{WO}_4)_4$.

Figure 4. Excitation spectra of $\text{Na}_5\text{Gd}_{1-x}\text{Eu}_x(\text{MoO}_4)_4$.

Figure 5. Excitation spectra of $\text{Na}_5\text{Gd}_{1-x}\text{Eu}_x(\text{WO}_4)_4$.

Figure 6. Excitation spectra of $\text{Na}_5\text{La}_{1-x}\text{Eu}_x(\text{MoO}_4)_4$.

Figure 7. Excitation spectra of $\text{Na}_5\text{La}_{1-x}\text{Eu}_x(\text{WO}_4)_4$.

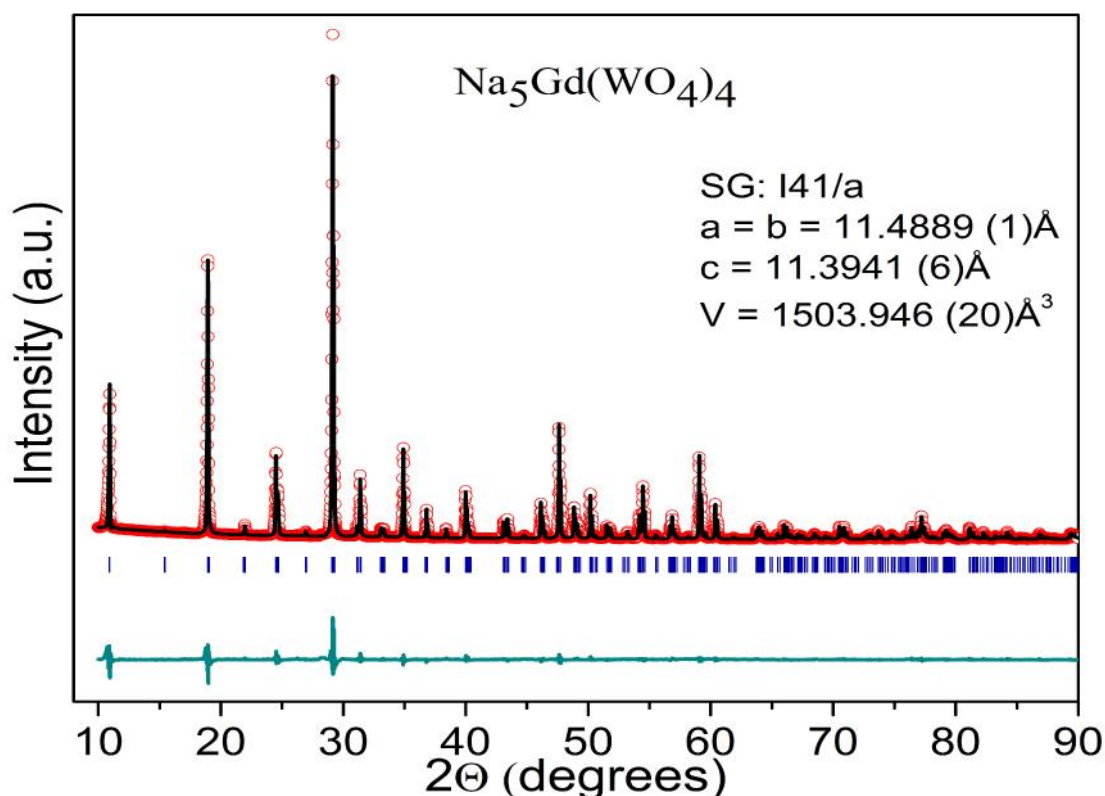


Fig1. X-ray powder diffraction patterns of $\text{Na}_5\text{Gd}(\text{WO}_4)_4$ (observed, calculated and difference patterns are represented with dots, bold line and solid line, respectively; positions of Bragg reflections with vertical bars).

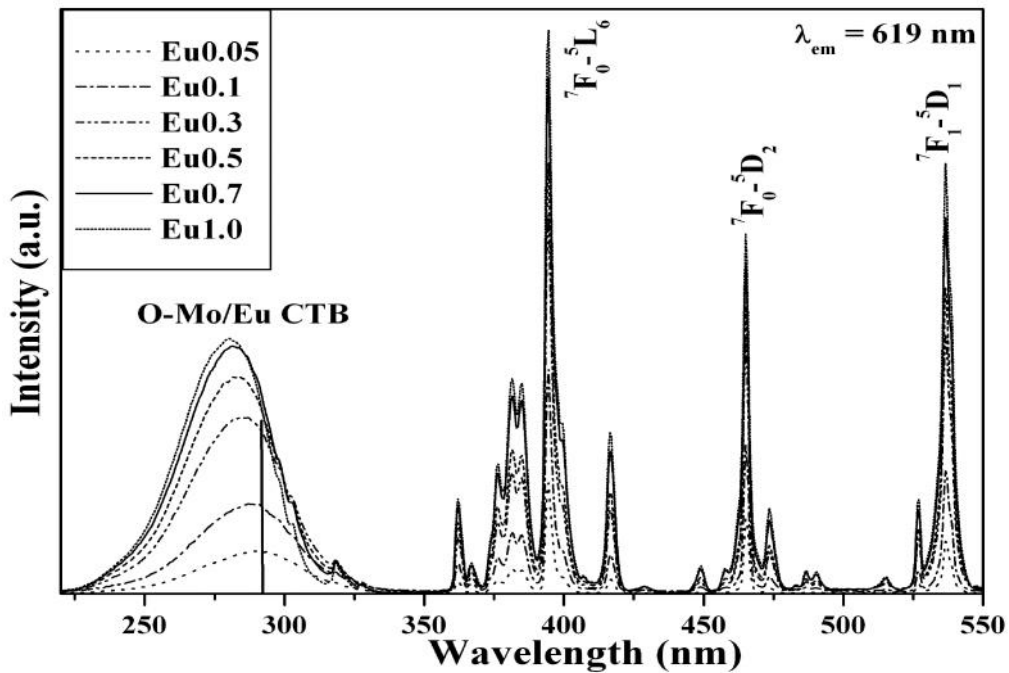


Fig2. Excitation spectra of $\text{Na}_5\text{Y}_{1-x}\text{Eu}_x(\text{MoO}_4)_4$.

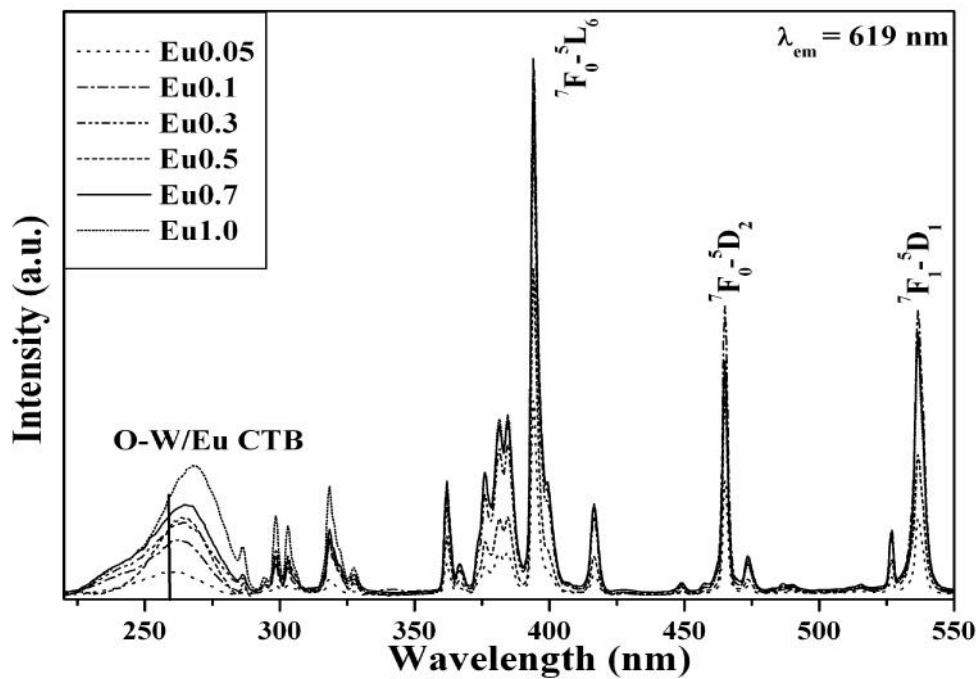


Fig3. Excitation spectra of $\text{Na}_5\text{Y}_{1-x}\text{Eu}_x(\text{WO}_4)_4$.

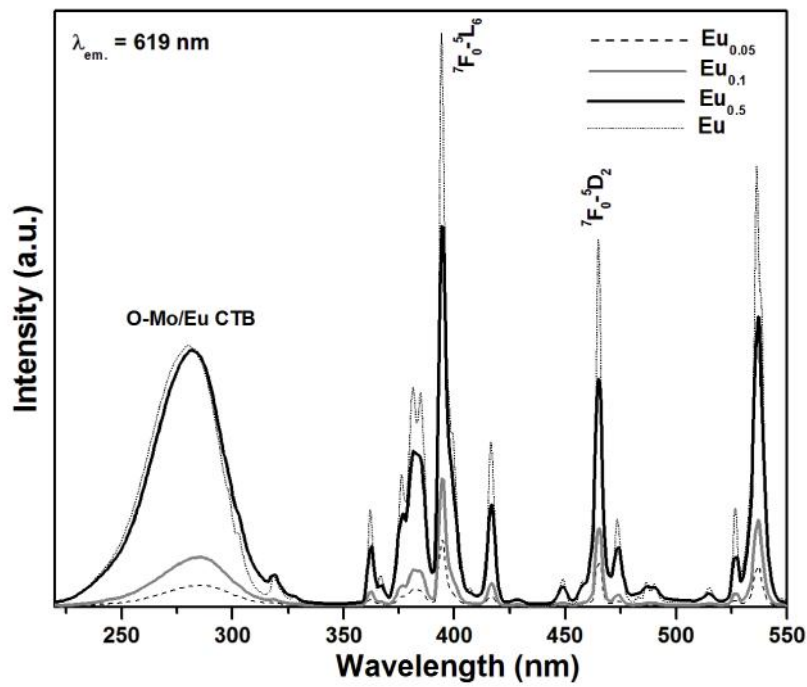


Fig. 4 Excitation spectra of $\text{Na}_5\text{Gd}_{1-x}\text{Eu}_x(\text{MoO}_4)_4$

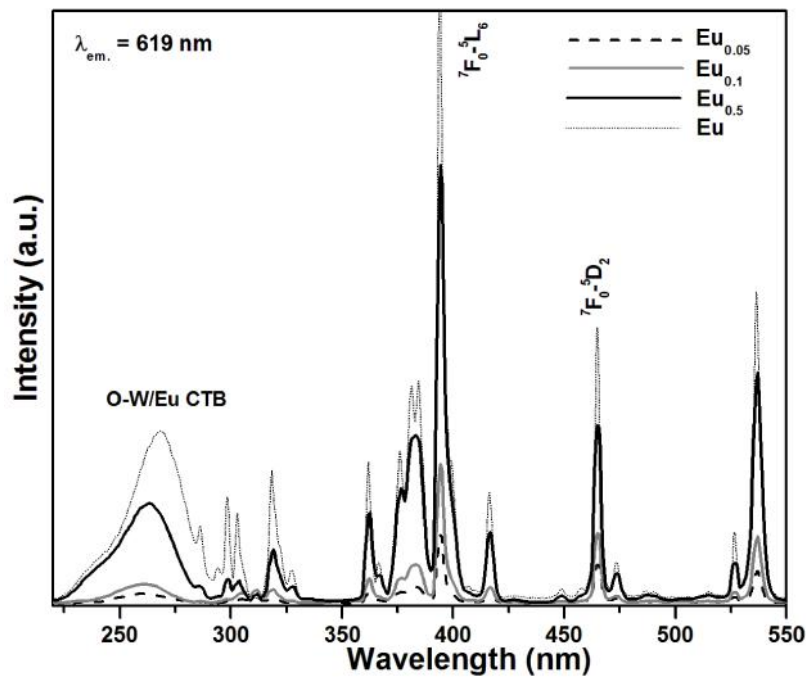


Fig. 5 Excitation spectra of $\text{Na}_5\text{Gd}_{1-x}\text{Eu}_x(\text{WO}_4)_4$

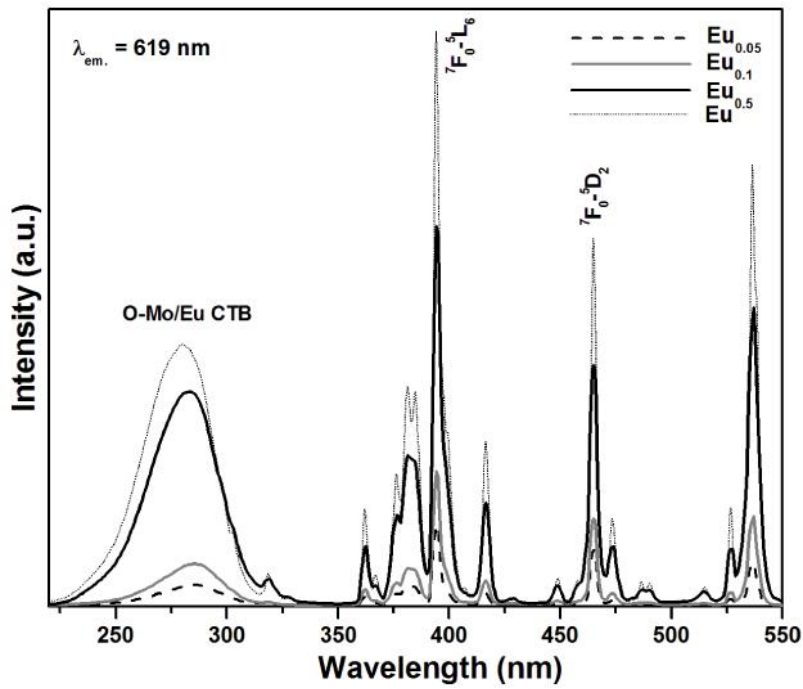


Fig. 6 Excitation spectra of $\text{Na}_5\text{La}_{1-x}\text{Eu}_x(\text{MoO}_4)_4$

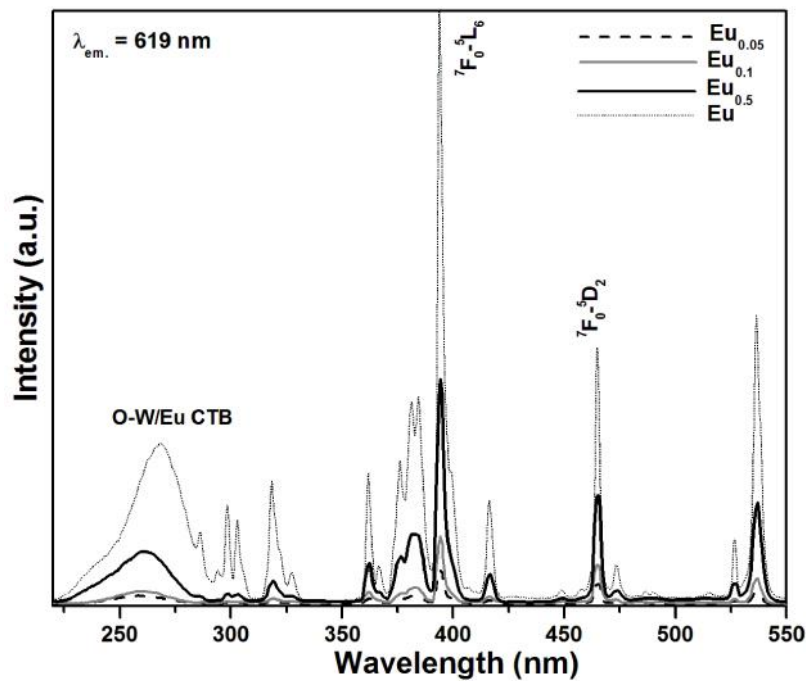


Fig. 7 Excitation spectra of $\text{Na}_5\text{La}_{1-x}\text{Eu}_x(\text{WO}_4)_4$

Table 1. Bond distances in Na₅Ln(MO₄)₄ (Ln = Y, Gd & La; M = Mo & W).

Na ₅ Y(MoO ₄) ₄	Na ₅ Y(WO ₄) ₄
Y-O – 2.3618(O2)Å 2.3664(O3)	Y-O – 2.3356(O2)Å 2.3577(O3)
Mo-O-1.7592(O1) 1.7752(O2) 1.7951(O3) 1.7408(O4)	W-O- 1.7770(O1) 1.8181(O2) 1.8108(O3) 1.7747(O4)
Na ₅ La(MoO ₄) ₄	Na ₅ La(WO ₄) ₄
La-O – 2.4949(O3) 2.4984(O4)	La-O – 2.4881(O3) 2.5073(O4)
Mo-O-1.7409(O1) 1.7622(O2) 1.7738(O3) 1.7890(O4)	W-O - 1.7515(O1) 1.7779(O2) 1.8006(O3) 1.7962(O4)
Na ₅ Gd(MoO ₄) ₄	Na ₅ Gd(WO ₄) ₄
Gd-O –2.4123(O1) 2.4151(O3)	Gd-O –2.4568 (O1) 2.4106 (O3)
Mo-O-1.8004(O1) 1.7426(O2) 1.7822(O3) 1.7700(O4)	W-O- 1.7885 (O1) - 1.8784 (O2) - 1.7729 (O3) -1.7735 (O4)